Supersonic Compression-Corner Applications of a Multiscale Model for Turbulent Flows

David C. Wilcox*
DCW Industries, Inc., La Cañada, California

The new "multiscale" model for turbulent flows developed by Wilcox has been subjected to a continuing series of rigorous applications, including shock-induced, boundary-layer separation, to test its accuracy in simulating complex flow phenomena. While previous applications have been inconclusive regarding superiority of the multiscale model over two-equation models, results obtained demonstrate a marked improvement in predictive accuracy for flows which include boundary-layer separation. As speculated in its original development, the model is superior because it accounts for disalignment of the Reynolds-stress-tensor and the mean-strain-rate-tensor principal axes.

I. Introduction

THIS paper includes results of three shock-separated turbulent boundary layer computations using both the multiscale and k-ω models developed by Wilcox.[1,2] In all cases, detailed comparisons with experimental data are presented. Flows considered include two planar Mach 3 compression-corner flows[3] and an axisymmetric Mach 3 compression corner flow.[4] The flows selected provide a definitive measure of differences attending use of the multiscale model compared to the k-ω model.

To underscore the significance of the results obtained in this study, it is worthwhile to briefly review our own efforts over the past 15 yr in quest of an acceptable numerical solution for flow into a compression corner. Wilcox[5] performed the first solutions to the Reynolds-averaged, Navier-Stokes equations using an advanced turbulence model for shock-induced separation of a turbulent boundary layer. This early computational fluid dynamics (CFD) study included six computations, three for reflection of an oblique shock from a flat plate and three for flow into a compression corner. Results of the study indicate that, using a two-equation turbulence model, a reasonably accurate description of the flowfield can be obtained for reflection of an oblique shock from a flat plate. However, the numerical flowfields for the compression corner cases differ significantly from the experimentally observed flowfields, even though Mach and Reynolds numbers and shock strength are identical to those of the flat-plate cases. Thus, a seemingly simple change in flow geometry causes a major difference in predictive accuracy.

To put these computations in proper perspective, note that the turbulence model used was the Saffman-Wilcox[6] k-ω^2 model with surface boundary conditions given by matching to the law of the wall, a procedure which has since come to be referred to as using wall functions. The numerical algorithm used was a first-order accurate, explicit, time-marching procedure. Since this study, computational methods have improved dramatically thanks to the innovative work of many researchers, most notably, MacCormack,[7] Beam and Warming,[8] and Steger[9]. Today, it is possible to perform two-equation turbulence model computations for shock-separated flows without the aid of wall functions on a (relatively crude) 1200-point finite difference mesh using a fast desk top microcomputer.[10] However, until this study, little improvement in predictive accuracy relative to our results of 1974 has been realized for compression corner flows.

The work of Horstman, et al.[11,12] provides clear substantiation of this claim. They have applied many turbulence models to shock-separated flows with almost universal results, viz 1) too little upstream influence as shown by pressure starting to rise well downstream of the measured beginning of adverse pressure gradient; 2) surface pressure in excess of measured values above the separation bubble; 3) skin friction higher than measured downstream of reattachment; and 4) velocity profiles downstream of reattachment which indicate flow deceleration in excess of corresponding measurements.

On the one hand, by using wall functions and the k-ϵ turbulence model,[13] Viegas, Rubesin and, Horstman[12] are able to remove item 3 from this list. On the other hand, they achieve only modest improvements in the other items. This lack of success on the compression-corner problem, which has persisted for more than a decade, is excellent testimony to the oft quoted statement that turbulence modeling is the pacing item in CFD.

Reference 5 conjectures that the relatively poor performance of the two-equation model for the compression corner computations is caused by the model's use of the Boussinesq approximation, which holds that the principal axes of the Reynolds stress tensor are parallel to those of the mean strain rate tensor. The physical reasoning is that, unlike the flow induced by an oblique shock reflecting from a flat plate, the mean strain rate tensor's principal axes abruptly rotate at the flat-plate/ramp junction. The Boussinesq approximation implies that the Reynolds stresses also change abruptly which, on physical grounds, would be a rather questionable event.

The excellent predictions made by Johnson[14,15] for transonic flow over a "bump" substantiate the notion that use of the Boussinesq approximation lies at the root of the two-equation model's inability to accurately simulate properties of separated flows. Using an approach in which a lag occurs between sudden changes in mean strain rate and the Reynolds shear stress, Johnson is able to duplicate measured flow properties to within engineering accuracy. His predictions are so much better than those obtained with the k-ϵ model that further applications with the latter seem pointless—especially since the k-ϵ model fares so poorly even for attached boundary layers in an adverse pressure gradient.[2] While Johnson offers significant improvement for transonic separated flows, the model has been demonstrated to be accurate for a limited range of Mach numbers and has been developed much in the spirit of mixing length, i.e., it is a very powerful "incomplete" model of turbulence.

Presented as Paper 88-0220 at AIAA 26th Aerospace Sciences Meeting, Reno, NV, Jan. 11-14, 1988; received Feb. 6, 1989, revision received July 11, 1989.

*President. Associate Fellow AIAA.

The primary purpose of this research study has been to apply both the multiscale and k-ω models to the three well documened separated flows referenced above and to assess the differences. As will be shown, the differences are profound.

II. Equations of Motion

All of the computations in this study have been done using both the multiscale and k-ω models. These models differ in the postulated constitutive relation between the Reynolds stress-tensor and mean-flow properties. The k-ω model implements the Boussinesq approximation in which Reynolds stress is assumed proportional to mean-strain rate. By contrast, the multiscale model computes each component of the Reynolds stress tensor individually. Complete details of the turbulence model equations are given in Refs. 1 and 2.

III. Applications

A. Numerical Procedure

Algorithm

The numerical algorithm used in the computations was developed by MacCormack[7] and has been used for many compressible separated flow computations by Hortsman, et al.[11,12,14] Because of its proven track record, we obtained the version of Horstman's program, which uses the k-ϵ turbulence model to describe the turbulence. After purging the k-ϵ model and incorporating the multiscale and k-ω models, we find that the modified program requires about 30% more memory than the original, primarily because of the additional arrays needed for the Reynolds stress components.

Turbulence Models

All computations have been done using both the k-ω and multiscale models. The k-ω model is far less complex than the k-ϵ model, mainly because of all the special viscous modifications needed to integrate the k-ϵ model through the sublayer. As a consequence, a computation using the k-ω model requires only 75% as much CPU time per time step as one using the k-ϵ model. The multiscale model requires approximately 50% more CPU time than the k-ω model. Thus, a computation using the multiscale model requires about 12% more CPU time per time step than a corresponding computation using the k-ϵ model.

Finite-Difference Grids

Dimensions of the computational domains for each case are listed in Table 1 in terms of the thickness of the incident boundary layer, δ_0. In all three computations, the finite-difference grid consists of 80 equally-spaced points between upstream and downstream boundaries, and 45 points lie between the lower and upper boundaries. The first 30 grid points normal to the surface extend to $y=\delta_0$; grid-point spacing increases in a geometric progression with a grading ratio between 30% and 35%. The remaining 15 points are equally spaced, covering the region from $y=\delta_0$ to the top of the grid.

Table 1 Primary flow and numerical parameters

Parameter	20 deg corner	24 deg corner	30 deg corner
Mach number	2.79	2.84	2.85
Total pressure (psf)	14,513	14,451	3,600
Total temp. (deg R)	464	472	513
Wall temp. (deg R)	493	497	487
B. L. thickness, δ_0 (ft)	.082	.075	.033
Mom. thickness, Re_θ	93,800	82,050	9,366
Shape factor, H	5.08	5.08	4.00
Grid length ($\Delta x/\delta_0$)	8	10	10
Grid height ($\Delta y/\delta_0$)	6	6	5
k-ω time steps	7,000	24,000	12,000
k-ω CPU time (min)	17	60	32
Multiscale time steps	7,000	40,000	12,000
Multiscale CPU (min)	25	138	45

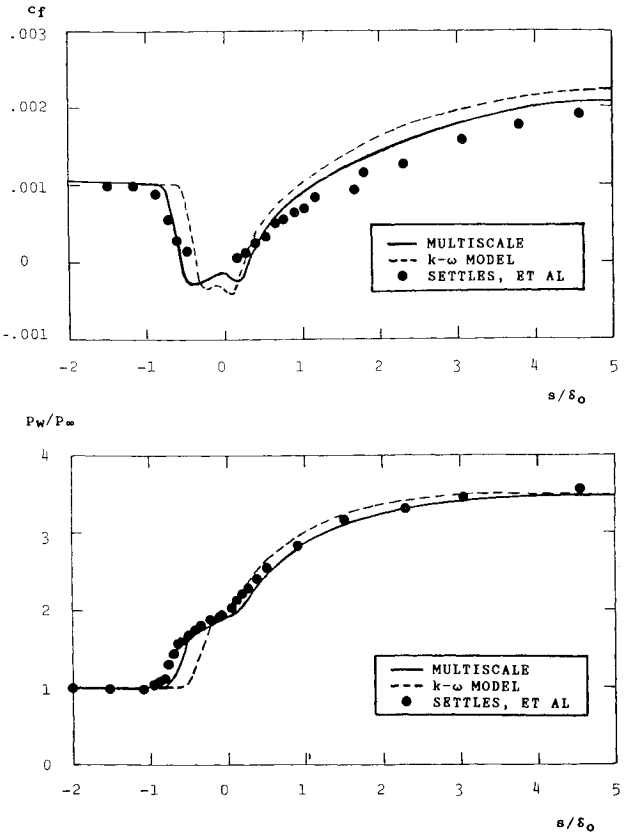

Fig. 1 Comparison of computed and measured skin friction and surface pressure for Mach 2.79 flow into a 20 deg compression corner; s is tangential distance from corner.

The mesh point closest to the surface lies below $y^+ = 0.7$ throughout the grid in all three cases. Upstream of the ramp, finite difference cells are rectangular. Downstream of the ramp, the cells are parallelograms aligned with the ramp.

Boundary and Initial Conditions

Upstream boundary conditions for the three computations have been obtained from a two-dimensional, boundary-layer program. We have been able to match the measured values of Re_θ and H for each case to within 1%. The upstream boundary-layer profiles have also been used as initial conditions throughout the computational domain.

Other Details

The equations of motion have been integrated through the sublayer with a viscous Courant number, $C_y = 2\nu\Delta t/(\Delta y)^2$ ranging between 30 and 90 for most of the computation and typically half this value for the final 25% of the computation to eliminate any possibility of solution dependence on the time step, a procedure recommended by MacCormack.[7] In every computation, a freestream fluid particle traverses the mesh at least 3 times and as many as 18 times. The relatively long run times are a direct consequence of having $y^+ < 1$, which was done to insure solution accuracy. Subsequent numerical experimentation has shown that having y^+ as large as 2 has little effect on solution accuracy with a significant reduction in CPU time.

IV. Applications

B. 20 deg Compression Corner

The first of the three applications is for Mach 2.79 flow into a 20 deg compression corner. This flow has been experimentally investigated by Settles, Vas and Bogdonoff[3] and includes a small region over which separation of the incident turbulent boundary layer occurs. Figure 1 compares computed and

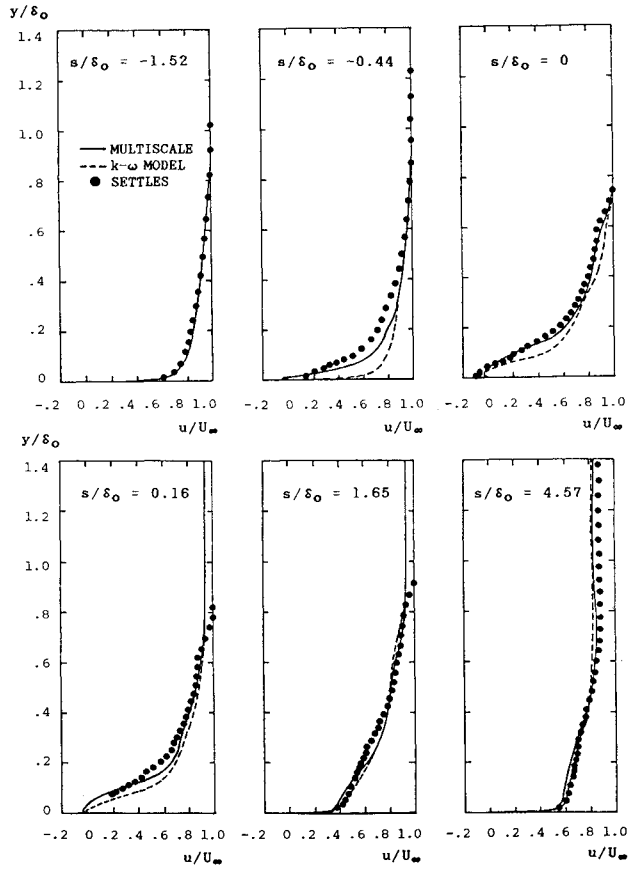

Fig. 2 Comparison of computed and measured velocity profiles for Mach 2.79 flow into a 20 deg compression corner; y is distance normal to the surface.

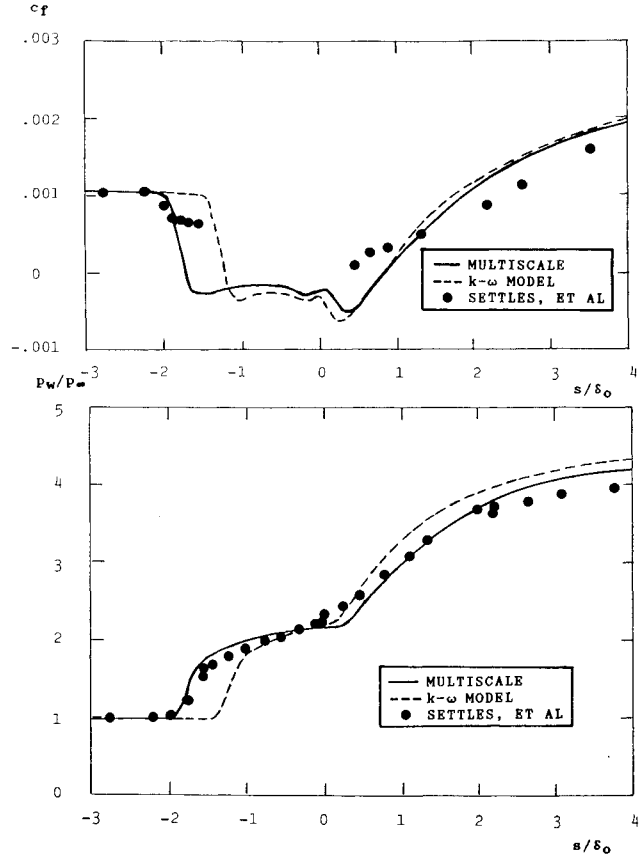

Fig. 3 Comparison of computed and measured skin friction and surface pressure for Mach 2.84 flow into a 24 deg compression corner; s is tangential distance from corner.

measured surface pressure p_w/p_∞ and skin friction, C_f. The multiscale model predicts more upstream influence, a lower pressure plateau at separation, and a more gradual increase in skin friction downstream of reattachment relative to the k-ω results. All of these features represent significant improvement in predictive accuracy. Figure 2 compares computed and measured velocity profiles throughout the interaction region. Multiscale model predictions are much closer to measured properties than k-ω model predictions—especially near the separation point. Using the k-ϵ model and specially devised wall functions, Viegas, Rubesin and Horstman[12] are able to achieve similar accuracy for this flow.

C. 24 deg Compression Corner

The second of the three applications is for Mach 2.84 flow into a 24 deg compression corner. This flow has also been experimentally investigated by Settles, Vas and Bogdonoff[3] and includes a larger region over which separation of the incident turbulent boundary layer occurs than in the 20 deg case of the preceding section. Figure 3 compares computed and measured surface pressure and skin friction. As in the 20 deg compression-corner computation, the multiscale model predicts much more upstream influence. Interestingly, the k-ω predicted pressure plateau at separation is very close to the measured level, and there is little difference between k-ω and multiscale predicted increase in skin friction downstream of reattachment. Figure 4 compares computed and measured velocity profiles throughout the interaction region. Again, multiscale model predictions are closer to measured properties than k-ω model predictions, most notably near the separation point.

Note that, for this flow, Viegas, Rubesin and Horstman[12] predict pressure plateau values about 20% higher than measured and are unable to simultaneously make accurate

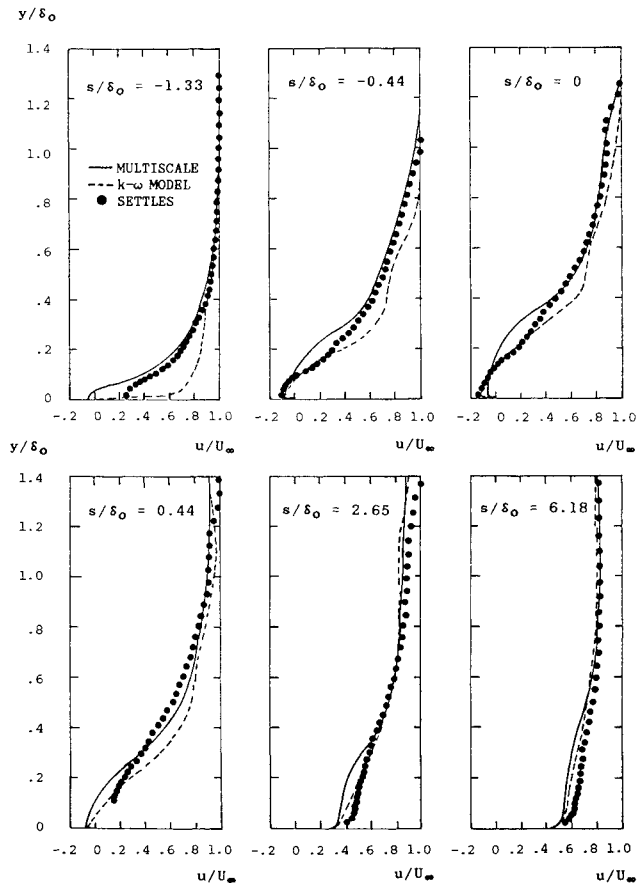

Fig. 4 Comparison of computed and measured velocity profiles for Mach 2.84 flow into a 24 deg compression corner; y is distance normal to the surface.

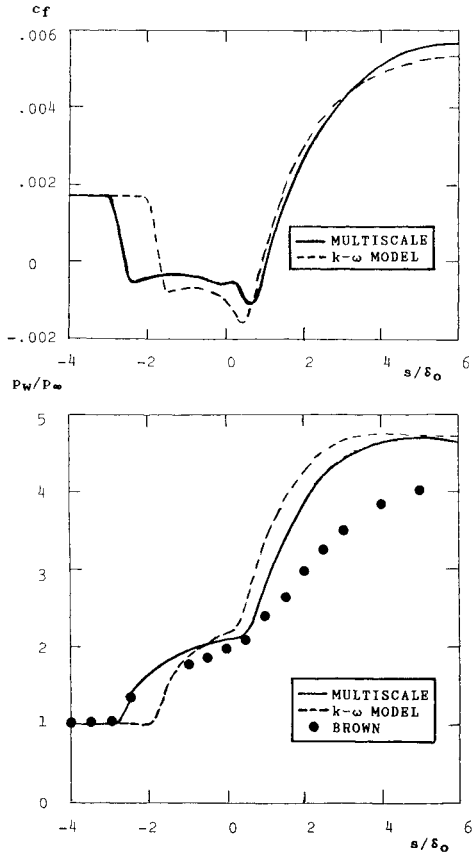

Fig. 5 Comparison of computed and measured skin friction and surface pressure for Mach 2.85 flow into a 30 deg compression corner; s is tangential distance from corner.

predictions for skin friction downstream of reattachment and the initial rise in surface pressure. That is, their solutions can match either skin friction or surface pressure, but not both.

D. Axisymmetric Compression Corner

Our third application is for Mach 2.85 flow into a 30 deg axisymmetric compression corner. This flow has been experimentally investigated by Brown[4] and includes a separation bubble of length comparable to the 24 deg planar compression corner. Figure 5 compares computed and measured surface pressure. Computed skin friction is also shown. Once again the multiscale model predicts much more upstream influence. For both models, the predicted pressure plateau at separation is about 10% higher the measured level, and there is little difference between k-ω and multiscale predicted increase in skin friction downstream of reattachment. The overall pressure rise is predicted by both models to be 4.7; whereas the measurements indicate a value of 4. The inviscid pressure rise for a 30 deg axisymmetric compression corner is 4.4 so that neither theory nor experiment appears to be completely consistent with the physics of this flow.

Figure 6 compares computed and measured velocity profiles throughout the interaction region. Multiscale model predictions are closer to measured properties than k-ω model predictions throughout the interaction region. Because of the stronger than measured overall pressure rise, the computed zero velocity line is more distant from the wall than measured and thus distorts the profiles somewhat.

In order to eliminate the possibility that the finite-difference grid is too coarse to provide an accurate computation for the freestream, the k-ω computation has been repeated with an 80×60 grid. In the refined grid, the same spacing is used for the boundary layer, and 30 equally spaced points cover the region from $y = \delta_0$ to $y = 5\delta_0$. No significant changes in the solution result from this mesh refinement.

E. Data Analysis

Results presented in the preceding subsections indicate that, for the three compression-corner cases considered, the multiscale model provides a flowfield more consistent with experimental observations than does the k-ω model. The primary reason for the difference in the two models' predictions can be found by examining predicted behavior of the Reynolds shear stress near the separation point. Figure 7 shows the maximum Reynolds shear stress τ_{max} throughout the interaction region for the three compression-corner computations. As shown, the k-ω model predicts a more abrupt increase in τ_{max} at separation and a much larger peak value than predicted by the multiscale model. For the axisymmetric case, the figure includes experimental data for points ahead of the measured separation point. As shown, the multiscale model τ_{max} falls within experimental data scatter.

The physical implication of the pronounced difference in the rate of amplification of the Reynolds shear stress is clear. Using the Boussinesq approximation, the k-ω model makes a far more rapid adjustment to the rotation of the mean strain rate tensor's principal axes than the multiscale model. Consequently, the predicted separation point and initial pressure rise lie closer to the corner with the k-ω model than measured. Predicting more physically realistic growth of the Reynolds stresses, the multiscale model predicts overall flow properties which are in much closer agreement with measurements.

It is interesting to note that for the multiscale model, although the pressure is in such close agreement with measurements, the numerical separation points are further upstream than indicated by oil flow measurements for all three compression corner cases. Table 2 summarizes computed and measured separation points. Careful examination of the numerical flowfields shows that a) the separation bubble is extremely thin near its leading edge and b) reverse flow velocities are very small in this extremely thin region. This behavior is best

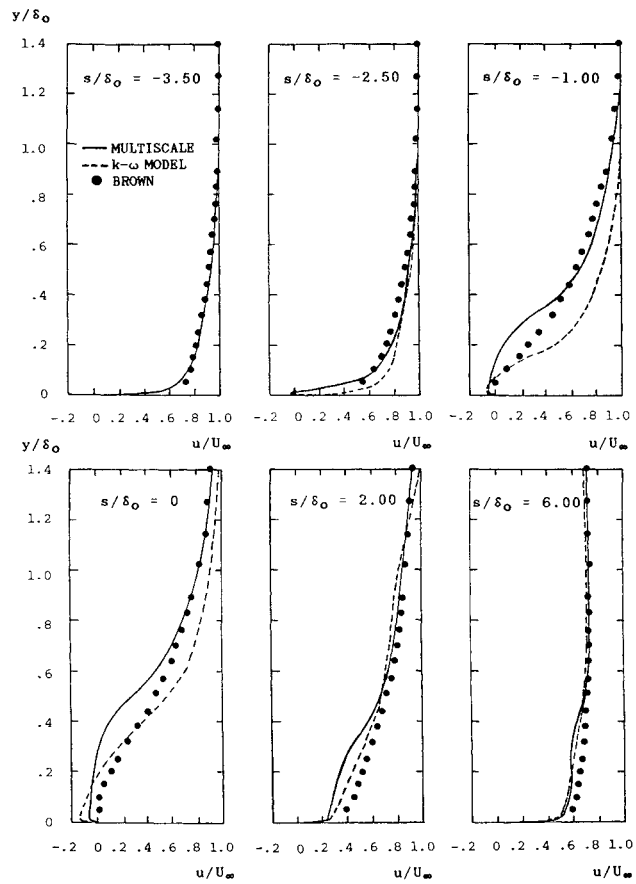

Fig. 6 Comparison of computed and measured velocity profiles for Mach 2.85 flow into a 30 deg compression corner; y is distance normal to the axis of symmetry.

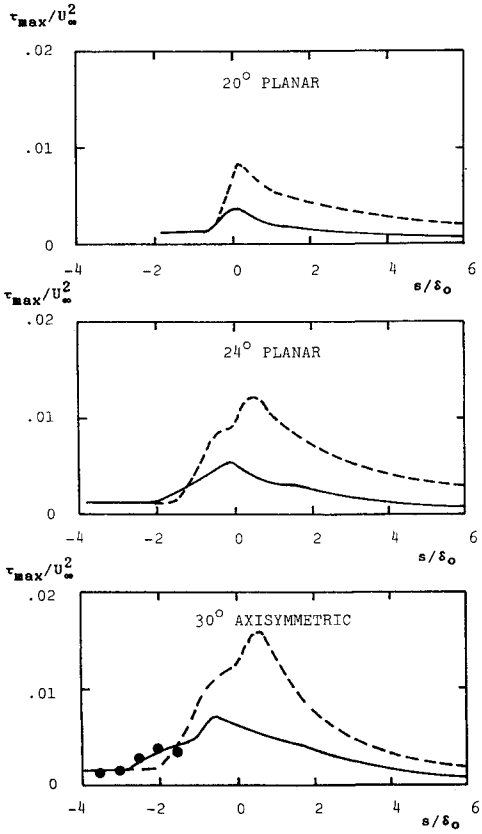

Fig. 7 Variation of peak Reynolds shear stress through the interaction region for the compression-corner computations; ———k-ω model; ——— multiscale model; ● Brown.[4]

Table 2 Computed and measured separation points

Case	Multiscale	k-ω	Measured
20°	−0.56	−0.38	−0.45
24°	−1.73	−1.23	−1.33
30°	−2.60	−1.70	−1.50

exemplified in Figs. 2 and 6. Specifically, the profile at $s/\delta_0 = -0.44$ in Fig. 2, and the profile at $s/\delta_0 = -2.50$ in Fig. 6; both show that the reverse flow portion of the numerical profile lies below the experimental data. Given the excellent agreement between computed and measured surface pressure, which is strongly influenced by separation bubble shape, the computed separation points appear more physically realistic than those indicated by the oil-flow measurements.

V. Summary and Conclusions

Three shock-separated flows have been numerically simulated using the mass-averaged, Navier-Stokes equations and both the k-ω and multiscale models. The multiscale model is clearly superior for supersonic compression corner flows, which is especially obvious in the vicinity of separation.

The multiscale model's superioriy over the k-ω model appears to be due to a more physically realistic description of the Reynolds stress tensor. Unlike the k-ω model, which uses the Boussinesq approximation that Reynolds stress is proportional to mean-strain rate, the multiscale model predicts a gradual increase in Reynolds shear stress near separation. Because the flow's effective resistance to separation is thus reduced, the separation point, and hence the initial rise in pressure, lies farther from the corner. Multiscale-model predicted surface pressure is much closer to measurements than the corresponding k-ω model surface pressure. Close agreement with limited experimental Reynolds shear stress data for the axisymmetric compression corner flow adds further verification that the multiscale model's predictions are physically sound.

On balance, the results obtained indicate that an important advance in the state of the art of separated-flow numerical simulation has been made. These results leave little doubt that continued use of turbulence models based on the Boussinesq approximation holds scant promise for accurate predictions. By contrast, the multiscale model, with only a 50% computational penalty per time step, brings numerical predictions into much closer agreement with the physics of separated flows.

Acknowledgments

Research was supported by the U.S. Army Research Office under Contract DAAL03-87-C-0004 with Thomas Doligalski as Contract Monitor. Partial funding for this study was also provided by James Wilson of the Air Force Office of Scientific Research. Computing time was made available by Joseph Marvin of the NASA Ames Research Center. C. C. Horstman of the NASA Ames Research Center contributed invaluable assistance as well as the computer program which served as the foundation for this study.

References

[1]Wilcox, D. C., "Multiscale Model for Turbulent Flows," *AIAA Journal,* Vol. 26, Nov. 1988, pp. 1311–1320.

[2]Wilcox, D. C., "Reassessment of the Scale Determining Equation for Advanced Turbulence Models," *AIAA Journal,* Vol. 26, Nov. 1988, pp. 1299–1310.

[3]Settles, G. S., Vas, I. E., and Bogdonoff, S. M., "Details of a Shock Separated Turbulent Boundary Layer at a Compression Corner," *AIAA Journal,* Vol. 14, 1976, pp. 1709–1715.

[4]Brown, J. D., "Two Component LDV Investigation of Shock Related Turbulent Boundary Layer Separation with Increasing Three Dimensionality," Ph.D. Thesis, University of California at Berkeley, 1986.

[5]Wilcox, D. C., "Numerical Study of Separated Turbulent Flows," AIAA Paper 74-584, 1974.

[6]Saffman, P. G., and Wilcox, D. C., "Turbulence-Model Predictions for Turbulent Boundary Layers," *AIAA Journal,* Vol. 12, April 1974, pp. 541–546.

[7]MacCormack, R. W., "A Numerical Method for Solving the Equations of Compressible Viscous Flow," *AIAA Journal,* Vol. 20, Sept. 1982, pp. 1275–1281.

[8]Beam, R. M., and Warming, R. F., "An Implicit Finite-Difference Algorithm for Hyperbolic Systems in Conservation Law Form," *Journal of Computational Physics,* Vol. 22, Sept. 1976, pp. 87–110.

[9]Steger, J., and Warming, R. F., "Flux Vector Splitting of the Inviscid Gasdynamics Equations with Application to Finite Difference Methods," NASA TM-78605, 1979.

[10]Wilcox, D. C., "Advanced Applications of the Multiscale Model for Turbulent Flows," AIAA Paper 87-0290, 1987.

[11]Viegas, J. R., and Hortsman, C. C., "Comparison of Multiequation Turbulence Models for Several Shock Boundary-Layer Interaction Flows," *AIAA Journal,* Vol. 17, Aug. 1979, pp. 811–820.

[12]Viegas, J. R., Rubesin, M. W., and Hortsman, C. C., "On the Use of Wall Functions as Boundary Conditions for Two-Dimensional Separated Compressible Flows," AIAA Paper 85-0180, 1985.

[13]Jones, W. P., and Launder, B. E., "The Prediction of Laminarization with a Two-Equation Model of Turbulence," *International Journal of Heat and Mass Transfer,* Vol. 15, 1972, pp. 301–314.

[14]Johnson, D. A., Hortsman, C. C., and Bachalo, W. D., "Comparison Between Experiment and Prediction for a Transonic Turbulent Separated Flow," *AIAA Journal,* Vol. 20, June 1982, pp. 737–744.

[15]Johnson, D. A., "Transonic Separated Flow Predictions with an Eddy-Viscosity/Reynolds-Stress Closure Model," *AIAA Journal,* Vol. 25, Feb. 1987, pp. 252–259.